

Development of High Voltage Pulse Power Supply for Dielectric Barrier Discharge (DBD) Plasma

Siti Norhamisah Rosdi¹, Norain Sahari^{1*}

¹Department of Electrical Engineering Technology, Faculty of Engineering Technology,
University Tun Hussien Onn Malaysia, 84600 Pagoh, Johor, MALAYSIA

*Corresponding Author Designation

DOI: <https://doi.org/10.30880/peat.2021.02.02.046>

Received 13 January 2021; Accepted 01 March 2021; Available online 01 December 2021

Abstract: In conventional DBD plasma, an AC power supply with a 50 Hz frequency is used to generate a high voltage in the DBD plasma reactor. However, the stable DBD plasma at air atmospheric pressure is difficult to achieve in low frequency power supply. Apart from that, a versatile power supply that can meet the various demand is essential. To generate plasma in DBD reactor, it is necessary to have a high frequency power supply. In this study, a portable and adjustable high voltage pulse power supply for DBD plasma generation is presented. The input driver circuit is designed by using two 555 timers to chop the electricity into pulse and then connected it to the ignition coil to step up the 12 DC voltage into 10 kV high voltage. The value of the capacitor and resistor was varied to study the effect on the output frequency of the pulse circuit by using Proteus simulation. The result shows that the simulation process has proven with the calculation to be right and yields the desired outcome based on the designed values. Then, the output of the high voltage pulse generator was compared with the simulation and hardware implementation. This high voltage pulse generator achieves its objective that can be used to generate DBD plasma at atmospheric pressure in the future study. Besides, it can replace the conventional pulse generator which used low frequency to generate high voltage.

Keywords: Dielectric Barrier Discharge (DBD) Plasma, High Voltage, Pulse Power Supply, Ignition Coil

1. Introduction

In recent years, non-thermal atmospheric plasma are intensively used in a wide range of research and industrial fields such as in aeronautics and aerospace, surface treatment processes, air and water pollutant reduction and biomedical applications [1][2][3][4]. DBD are often used as non-thermal plasma sources because they allow the generation of homogeneously distributed non-thermal plasma at atmospheric pressure in a cheap way. DBD plasma is typically obtained between two parallel electrodes

(plate type and coaxial cylinder type) separated by a gap of some millimeters and excited by alternating current (AC) voltage with frequency in the range of 1-20 kHz [5].

Otto et al. made important contributions to the development of industrial ozone generators utilizing DBD [1]. These novel applications of DBD have reached market values substantially at least ten times higher than the first ozone market. For many decades, ozone and nitrogen oxide formation in DBD become an important investigation. At the beginning of the 20th century, Warburg conducted extensive laboratory investigations on the nature of the silent discharge [6].

To generate plasma in DBD reactor, it is necessary to have a high voltage power supply. When a variable voltage, with high enough amplitude is applied to the electrodes, the gas breakdown occurs. This gas breakdown can be a threshold for plasma occur. Significant attention has been given to the design and production of the pulsed power supplied, due to the importance of the excitation sources for the discharge characteristics of DBD and the application effect. Because of the various applications of high voltage pulsed power, a large number of pulsed generators were studied and realized [7].

In this paper, the construction of a portable and adjustable high voltage pulse power supply at variable frequency has been proposed to obtain DBD plasma at atmospheric pressure in the future. The development of a high voltage pulse generator with the simulation result is provided. Finally, the measurement result of the hardware pulse generator with different frequencies and the pulse width were presented.

The range for high voltage generation that will cover for this project is limited to 10 kV. Then, the high voltage pulse generator circuit will be analyzed by using Proteus 8 Simulation. This project is focused on the power supply construction and the output produced on the ignition coil.

2. Materials and Method

This section will explain the development of high voltage pulse generator that started with the simulation of timing circuit by using Proteus Simulation. The timing circuit was adjusted in order to achieve the required objective. After simulation process have been fulfilled and satisfied with the result generated, it moves to the hardware implementation. The operation of each types of components also presented.

2.1 Flow Chart

In this project, the timing circuit which is pulse generator is used to energize the ignition coil. Ignition coils need a pulse generator to be operated under DC supply in order to generate high voltage. This power supply can work over the range of 1 kHz to 100 kHz. The elements of the high frequency power supply as shown in Figure 1.

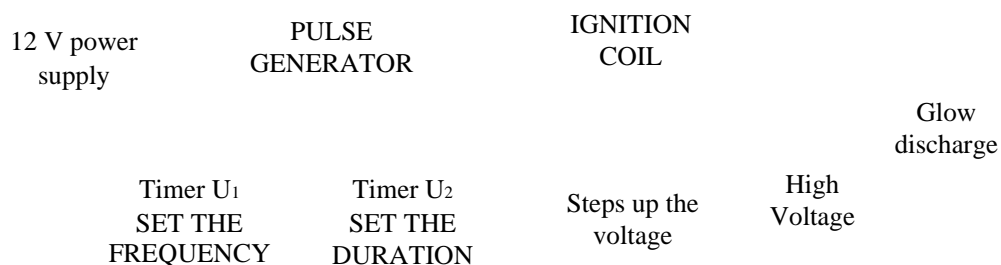


Figure 1: Elements of the high frequency power supply

The flowchart in Figure 2 shows the project planning to ensure the whole project works smoothly and successfully to achieve the aim and objective.

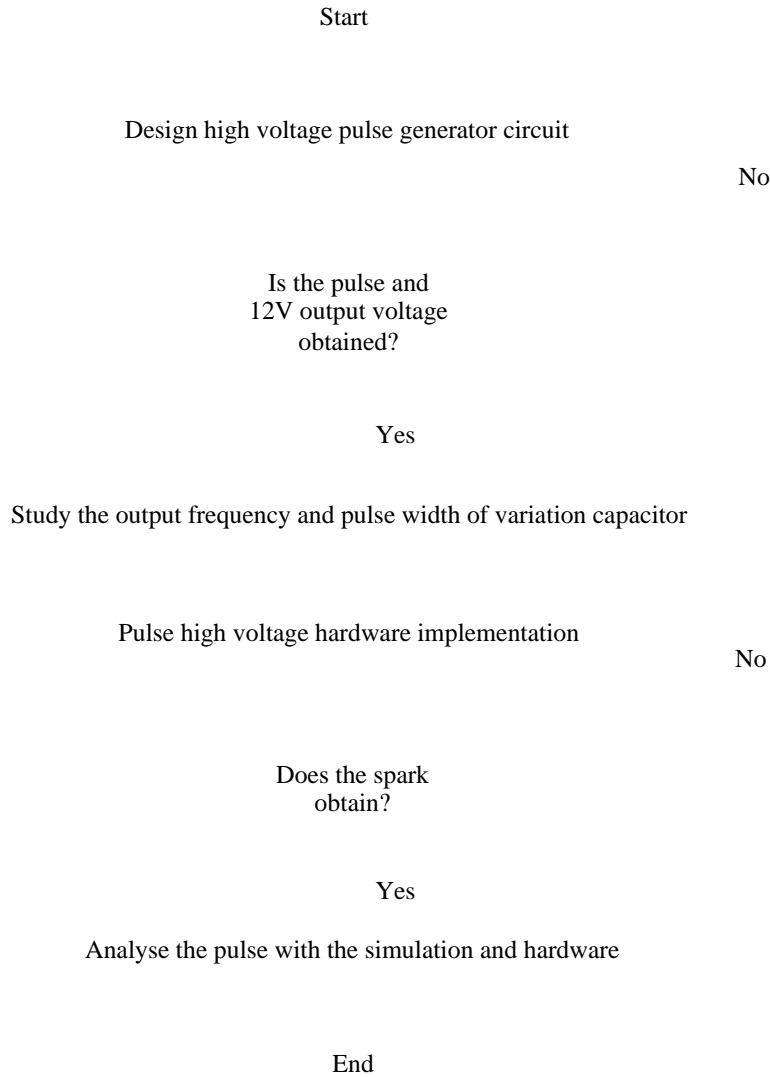


Figure 2: Flowchart for overall project

2.2 Hardware development

Table 1 shows the list of the component required in the circuit with their specification.

Table 1: List of components

Component	Description
NE555 timer (U ₁ and U ₂)	U ₁ operate in stable mode, U ₂ operate in mono-stable mode
Capacitor (C ₁ and C ₂)	1 μF, 0.1 μF and 0.01 μF
Power MOSFET	IRFZ44N
Resistor	180 Ω, 330 Ω, 1 kΩ, 10 kΩ, 2.2 kΩ, 4.7 kΩ
Variable resistor (RV ₁ and RV ₂)	50 kΩ
Diode	1N4004
Battery	12 V

2.3 Circuit of pulse generator

Figure 3 shows the complete schematic circuit for high voltage pulse generator power supply. In this study, 12 V power is required as a DC power supply to turn on the pulse generator circuit. The circuit is designed by using two NE555 timers to chop the electricity into pulses. In the first NE555 timer, U_1 determines how often the pulses occur, and C_1 acts as the timing capacitor for the timer. While the second NE555 timer, U_2 determines the duration of pulse it produces during ON state and C_2 is the timing capacitor for the timer.

For better clarification, the construction of the pulse generator consists of two parts; the first part is determining the frequency of the pulse generated and the second part determines the pulse width. The different values of selected capacitors give a different result of the output frequency of the circuit. Both timer U_1 and U_2 consist of 50 k Ω potentiometers. The timing parameters of the resulting pulses changes by adjusting both potentiometers. It allows us to fine tune the pulse generator within the timing range of the selected capacitors.

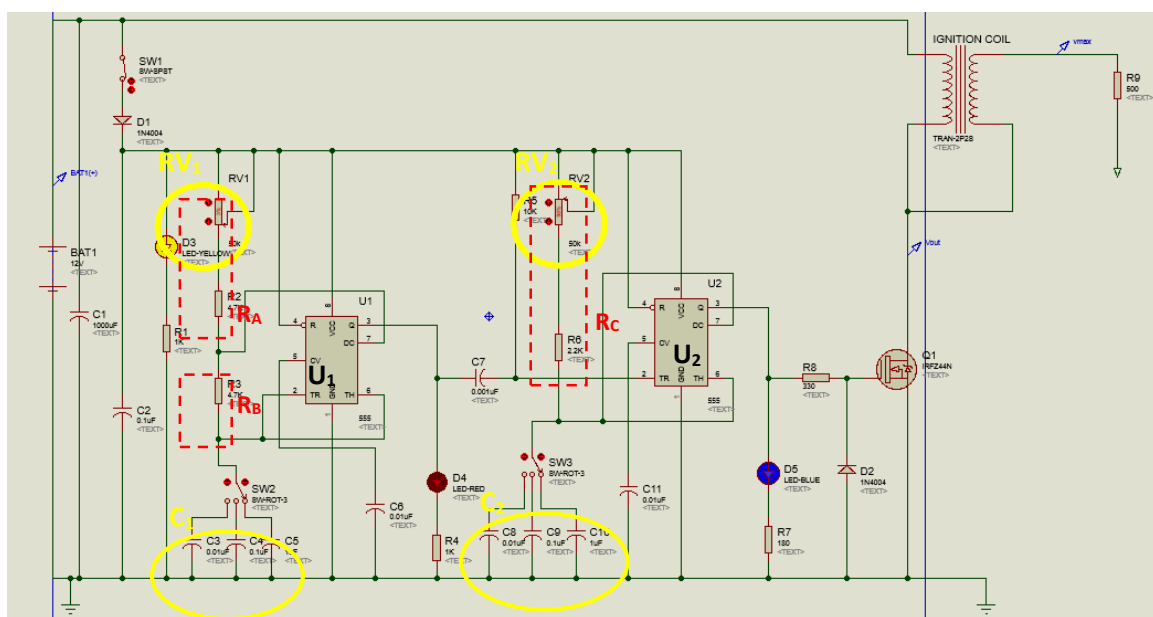


Figure 3: Schematic diagram of pulse generator in Proteus Simulation

An ignition coil is used at the end of the energizer to boost the voltage of the pulses. In this study, one of a driver circuit will be operated directly under DC supply at 12 V source to energize the ignition coil. The driver circuit is needed so that the ignition coil can be operated just like a transformer in order to produce high voltage. The DC current flow will increase through the primary when the switch is closed. It will produce a magnetic field inside the iron core where the energy is stored. The current is sudden interrupted when the switch is open. Then the magnetic field collapses and releasing the stored energy in the form of a large voltage pulse. The resulting of the peak voltage up to 10 kV is achieved by multiplying the voltage pulse to the turn ratio. In the circuit, the transformer with a coupling of 0.999 with turn's ratio of 1:100 is set. The supply voltage of the ignition coil will step up the output voltage over the range of 10 kV. It will produce a variety of voltages with different frequencies. In this design, Bosch induction coil is used with the primary inductance 1 H and secondary inductance 694 kH.

2.4 Design calculation

- Configuration equation in a stable mode (U_1)

Frequency and duty cycle are depending on the value of resistors and external capacitor that will be used to adjust the charging and discharging times.

The charge and discharge time are given by:

$$t_c = 0.693(R_A + R_B)C \quad \text{Eq. 1}$$

$$t_d = 0.693(R_B)C \quad \text{Eq. 2}$$

Thus, the total period and frequency are defined as:

$$T = t_c + t_d = 0.693 (R_A + 2R_B)C \quad \text{Eq. 3}$$

$$f = \frac{1}{T} = \frac{1.44}{(R_A + 2R_B)C} \quad \text{Eq. 4}$$

The percentage of duty cycle, as a fraction of total period that the output is high, is:

$$D = \left(\frac{R_A + R_B}{R_A + 2R_B} \right) \times 100 \quad \text{Eq. 5}$$

- Configuration equation in monostable mode (U_2)

The resistor in this system was set to be variable so that it can be adjusted to a desired result. For this mode of operation, R_C and external capacitor are related to each other as depicted in equation below.

The time when the output stays high is given by:

$$t_h = 1.1 \times R_C \times C \quad \text{Eq. 6}$$

- Configuration equation ignition coil output

This ignition coil contains iron core and operated like a step-up transformer where the output voltage in the range of 10 kV. The secondary voltage is related on the value of primary inductance (L_P) and secondary inductance (L_S).

Output voltage step-up design:

$$V_{secondary} = \sqrt{\frac{L_S}{L_P}} (V_{primary}) \quad \text{Eq. 7}$$

3. Results and Discussion

In this section, the results produced from the high voltage pulse power supply will be analyzed. The analysis will be started on circuit analysis using Proteus Simulation. The comparison on the effect of capacitors and resistors value variation that connected to NE555 timer to the output frequency will be presented. These results will be used as guidance for hardware implementation.

3.1 Calculation Results

Before fabricating the hardware, the simulation process needs to be completed first to reduced human error in designing the circuit. The simulation process can be done easily when the passive components are determined first in the simulation parameters. For that purpose, equation (1)-(7) were executed to obtain those values. All the calculated values are shown in Table 2, Table 3 and Table 4.

Table 2: Calculated values for R_A , R_C , and C_I in frequency (First timer, U_1)

Frequency, f (Hz)	Duty cycle, D (%)	$R_A(\Omega)$	$R_B(\Omega)$	C_I (F)
22.46 – 102.13	92.67	54.7k	4.7k	1 μ
224.6 – 1.02 k	92.67	54.7k	4.7k	0.1 μ

2.246 k – 10.21 k	92.67	54.7k	4.7k	0.01 μ
<i>*R_A is made variable to adjust the frequency</i>				

Table 3: Calculated values for R_C, and C₂ in pulse width (second timer, U₂)

Pulse Duration (s)	R _C (Ω)	C ₁ (F)
0.057	52.2k	1 μ
5.742m	52.2k	0.1 μ
0.5742m	52.2k	0.01 μ
<i>*R_C is made variable to adjust the pulse width</i>		

Table 4: Parameters of calculated value for both NE555 timer

Passive Component	Timer U ₁ (astable)	Timer U ₂ (monostable)
R _A (Ω)	54.7 k	-
R _B (Ω)	4.7 k	-
R _C (Ω)	-	52.2 k
C1 & C2 (F)	1 μ , 0.1 μ , 0.01 μ	1 μ , 0.1 μ , 0.01 μ
<i>*R_A and R_C are made variable to adjust the frequency and pulse width</i>		

Based on Table 2, the frequency of the pulse generator will increase when the value of the capacitor decreases. If potentiometer (RV₁) is reduce to the minimum value, the frequency of the pulse generator will increase. While in Table 3, the duration of pulses will longer by increasing the value of capacitor. If potentiometer (RV₂) is reduce to the minimum value, the pulse generator during ON state will short.

The result obtained from the simulation was validated by comparing it with the calculation from the pulse generator circuit. The circuit completely depends on the value of the capacitor and resistor network in Table 4 for variation of pulse frequency and pulse duration.

3.2 Circuit analysis using Proteus Simulation

A complete circuit of pulse generator as shown in Figure 3 was tested using different values of the capacitor. The different selected capacitors give a different result of the output frequency of the circuit. Based on the simulation results, the proposed circuit was successful in generating the desired output. That means the theoretical concept of this pulse generator has been proved right.

Figures 4 (a) and (b) show the simulation result of the input and output voltage when 12 VDC supply the voltage to turn on the pulse generator circuit. The circuit is designed by using two NE555 timers to chop the electricity into pulses. IRFZ44N power MOSFET in this circuit acting as a switch that can be turned on or turned off when the voltage is supplied in the pulse generator circuit. The output result in Figure 4(a) was obtained before connecting to the ignition coil where 12 VDC converted into the pulses. Then the pulse generator circuit will operate to energize the ignition coil in order to produce high voltage. The supply voltage of the ignition coil will step up the output voltage over the range of 10 kV as shown in Figure 4(b).

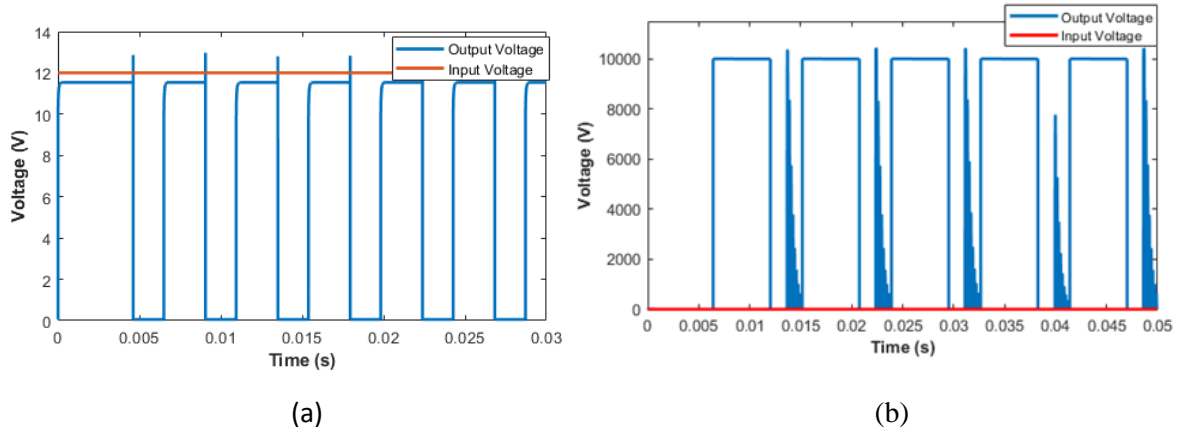


Figure 4: Input and output voltage (a) before ignition coil (b) after ignition coil

3.2.1 Output frequency of pulse generator circuit

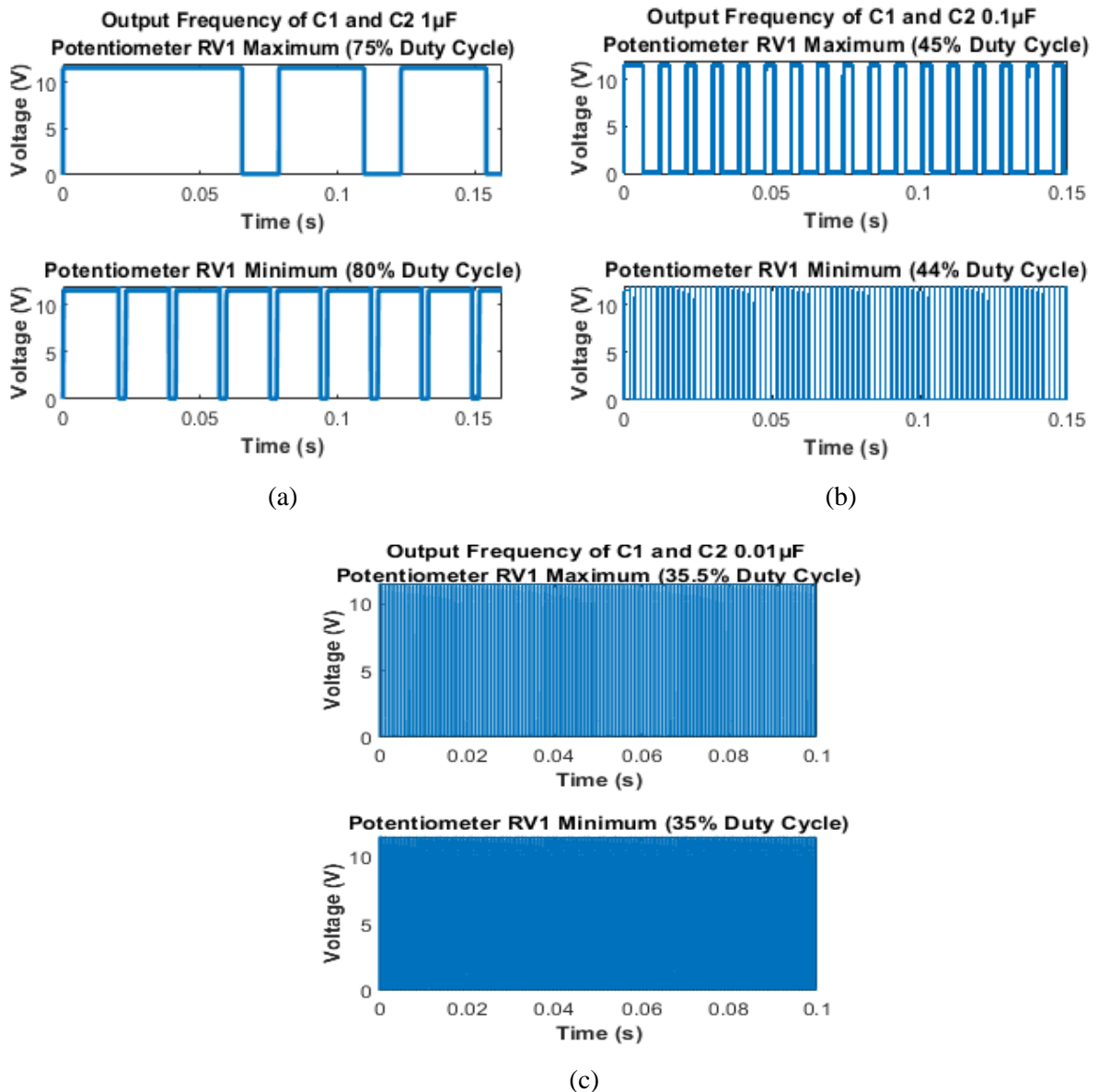


Figure 5: Output waveform for C_1 and C_2 equal to (a) 1 μ F, (b) 0.1 μ F, and (c) 0.01 μ F when varies the potentiometer of RV_1

Both timer U_1 and U_2 consist of $50\text{ k}\Omega$ potentiometers. The timing parameters of the resulting pulses changes by adjusting these potentiometers. Figure 5 shows the output frequency waveform obtained by varies the potentiometer RV_1 decreases from maximum to minimum value by altering the capacitor (C_1 and C_2) value with $1\ \mu\text{F}$, $0.1\ \mu\text{F}$ and $0.01\ \mu\text{F}$. The number of pulses produce is increases per second when varies the potentiometer to the minimum value compared to the maximum value. As clearly be shown, the number of pulses is increased by applied the $0.01\ \mu\text{F}$ followed by the $0.1\ \mu\text{F}$ and $1\ \mu\text{F}$. This is because the capacitive reactance of each capacitor is inversely proportional to frequency. The smallest value of capacitor gives lower pulse duration and higher output frequency.

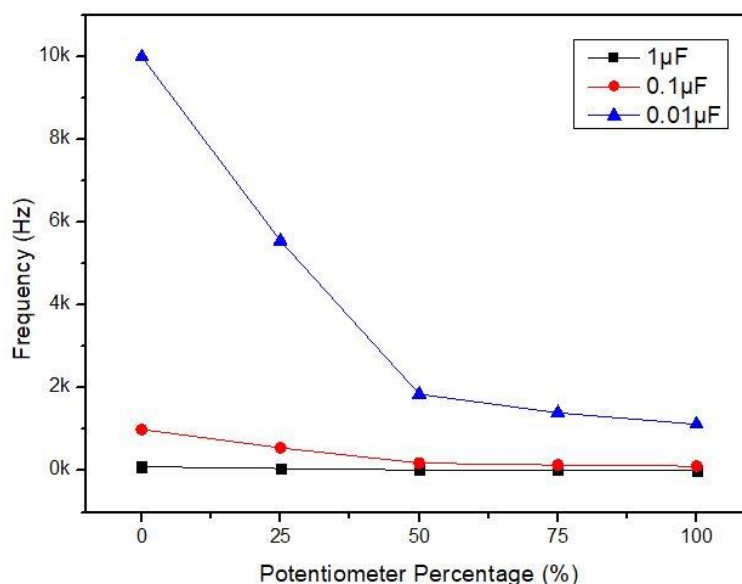


Figure 6: The output frequency of C_1 and C_2 when varies the potentiometer percentage

That means the frequency will high in timer U_1 while the duration of the pulse will short in timer U_2 when the value of the potentiometer is varied to the minimum value. The detail of simulation results for the output frequency waveform was summarized in Figure 6 and Table 5. The value of C_1 and C_2 with both range pulse frequency and pulse duration was recorded.

Table 5: Pulse frequency and pulse duration of capacitor C_1 and C_2

Pulse frequency	C_1 and C_2	Pulse Duration
11.24 Hz to 100 Hz	$1\ \mu\text{F}$	10 ms to 89 ms
112.4 Hz 1 kHz	$0.1\ \mu\text{F}$	1 ms to 8.9 ms
1.124 kHz to 10 kHz	$0.01\ \mu\text{F}$	100 μs to 0.89 ms

3.2.2 Pulse width of the generator

Figure 7 displays the simulation result for pulse duration of $1\ \mu\text{F}$, $0.1\ \mu\text{F}$, and $0.01\ \mu\text{F}$ capacitor. The pulse width of the output generator was adjusted by altering the value of the potentiometer RV_2 to the maximum value without affecting its frequency. Based on Figure 7, the duration of the pulse generator during the ON state will longer if the value of RV_2 is increasing.

For the duty cycle, it can be varied by adjusting the potentiometer RV_2 . The duty cycle will increase when the output time stays high is longer and the value of potentiometer RV_2 is increasing. As can be shown in the Figure 7, the duration of pulses will longer by increasing the value of capacitor $1\ \mu\text{F}$ followed by the $0.1\ \mu\text{F}$ and $0.01\ \mu\text{F}$. The pulse produced may have a period of seconds or may have a duration as short as microseconds.

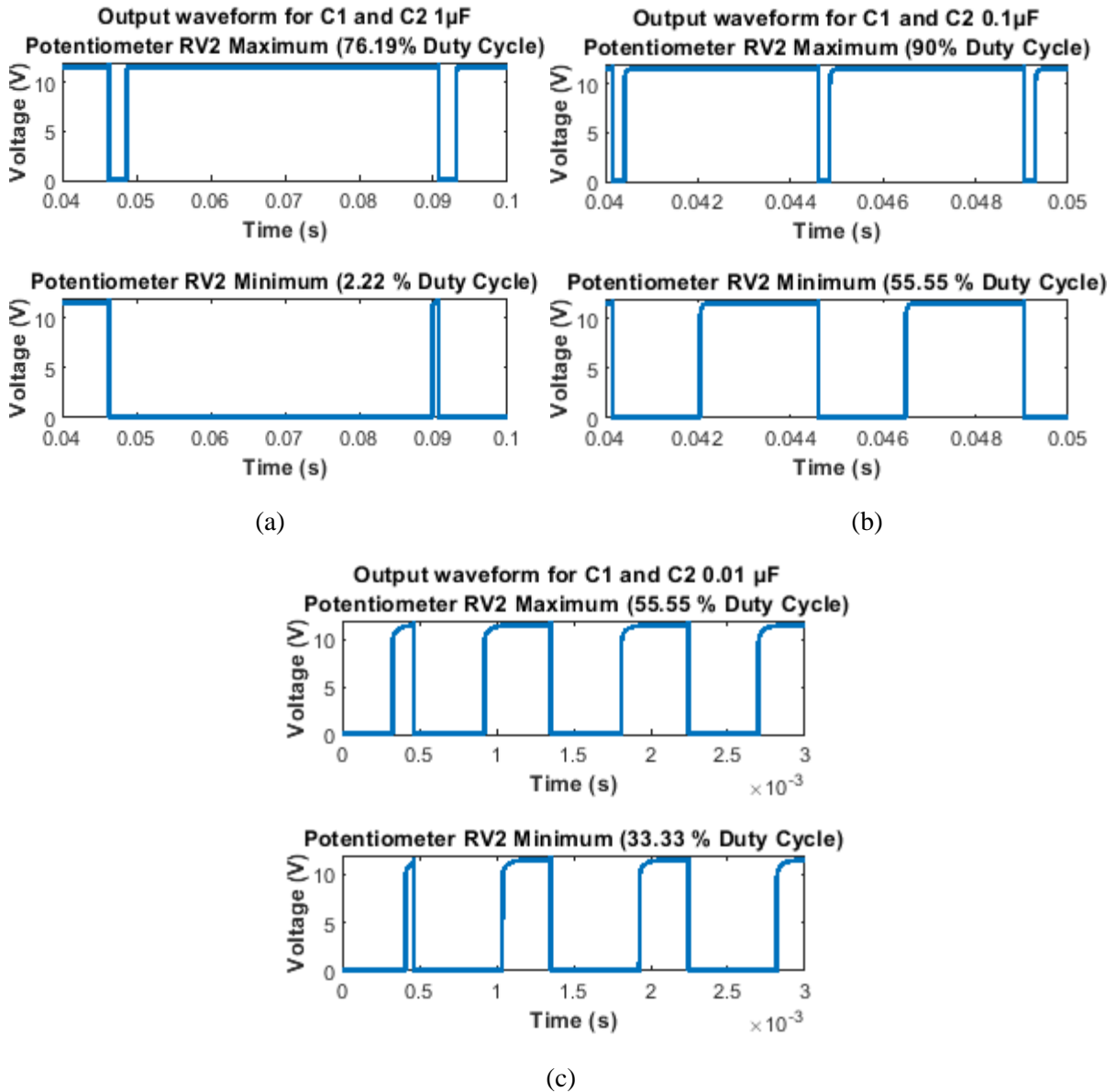


Figure 7: The simulation result for C₁ and C₂ equal to (a) 1 μF (b) 0.1 μF, and (c) 0.01 μF when varies the potentiometer RV₂

3.2.3 Output ignition coil of the pulse generator

Figure 8 shows the simulation result of the output energizer impulse voltage that successfully achieved over the range 10 kV. The frequency and pulse duration are different depending on the variation of a capacitor used. The noise obtained in between the on and off time of the pulse waveform is might be due to the high voltage spark ignited at the end of the output.

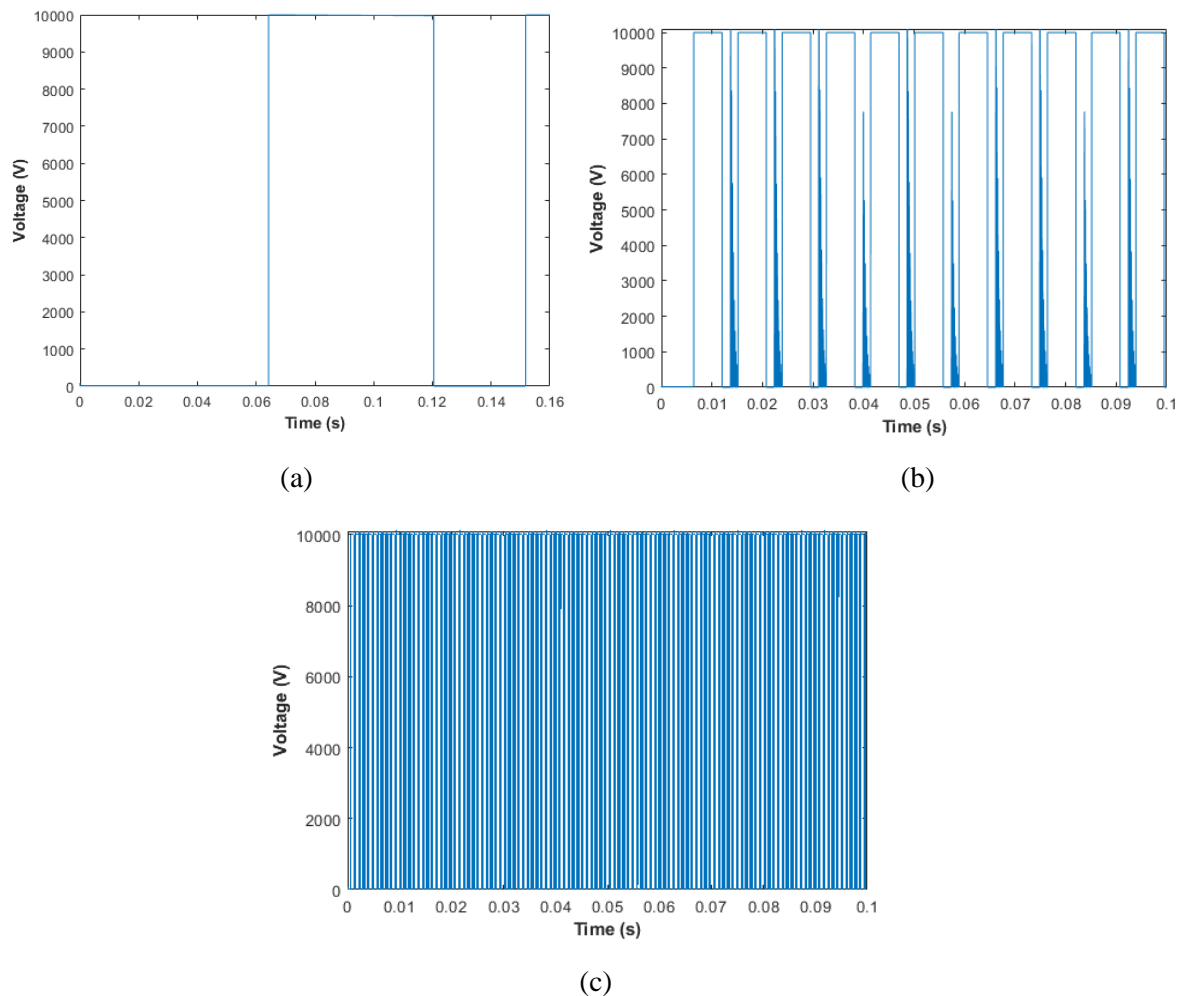


Figure 8: Output energizer of impulse voltage for C_1 and C_2 equal to (a) $1 \mu\text{F}$, (b) $0.1 \mu\text{F}$, and (c) $0.01 \mu\text{F}$ respectively.

3.3 Experimental Results for hardware implementation

The hardware implementation is shown in the Figure 9 and was supplied with 12 VDC battery. It also equipped with two NE555 timers to chop the electricity into pulse and then connected it to the ignition coil to step up the 12 VDC voltage into 10 kV high voltage. All parameters values in Table 3 were implemented in the experimental test and simulation process. The output voltage of the experimental setup was measured by using oscilloscope and was validated by comparing it with the simulation result.

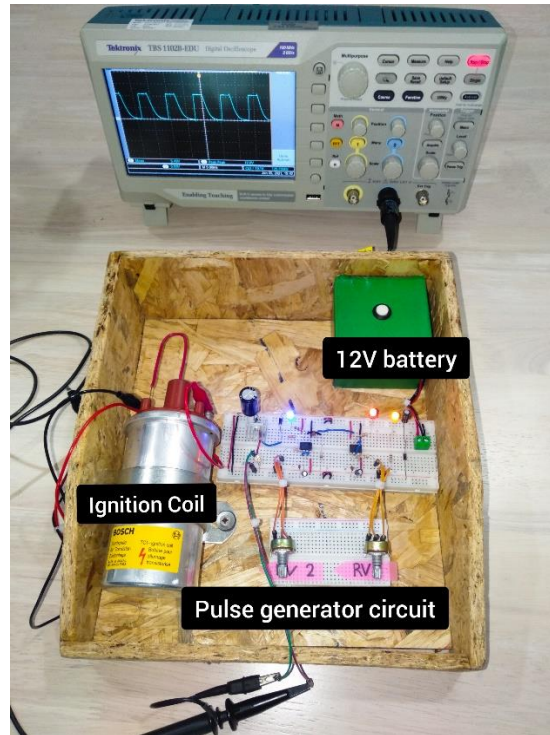


Figure 9: A complete fabrication of pulse generator

The output pulse from the driving circuit is fed into negative terminal of the ignition coil as shown in Figure 10. The inset is the magnification of output pulse produced at the high voltage terminal of ignition coil. As can be seen clearly, the spark is produced on the output ignition coil. That means the voltage obtained by the circuit is enough high to energize the ignition coil. This is because the spark will be produced when the voltage is greater than 10 kV. The pulse produced from the ignition coil may have a period of seconds or may have a duration as short as microseconds. The output result completely depends on the capacitor and resistor network for variation of pulse frequency and pulse duration.



Figure 10: Output energize of the ignition coil

Figure 11 shows the experimental result of the pulse generator when the potentiometer RV_1 varies from maximum value to the minimum value by altering the capacitor (C_1 and C_2) with $1\ \mu\text{F}$, $0.1\ \mu\text{F}$ and $0.01\ \mu\text{F}$. As clearly be seen, the number of pulses produce is increases per second when varies the

potentiometer to the minimum value compared to the maximum value. The result obtained means that the frequency will high for the lowest value of capacitors used.

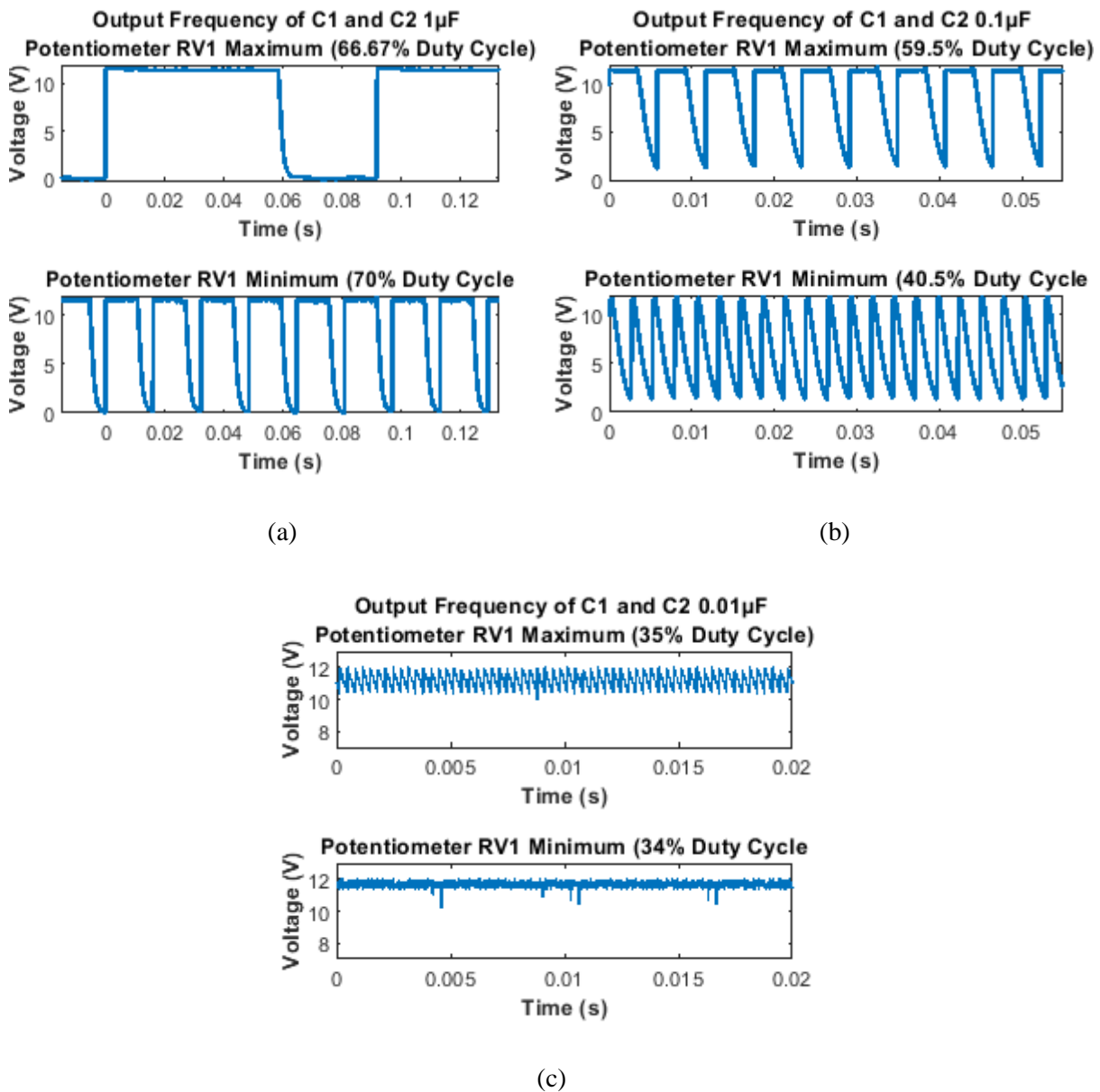
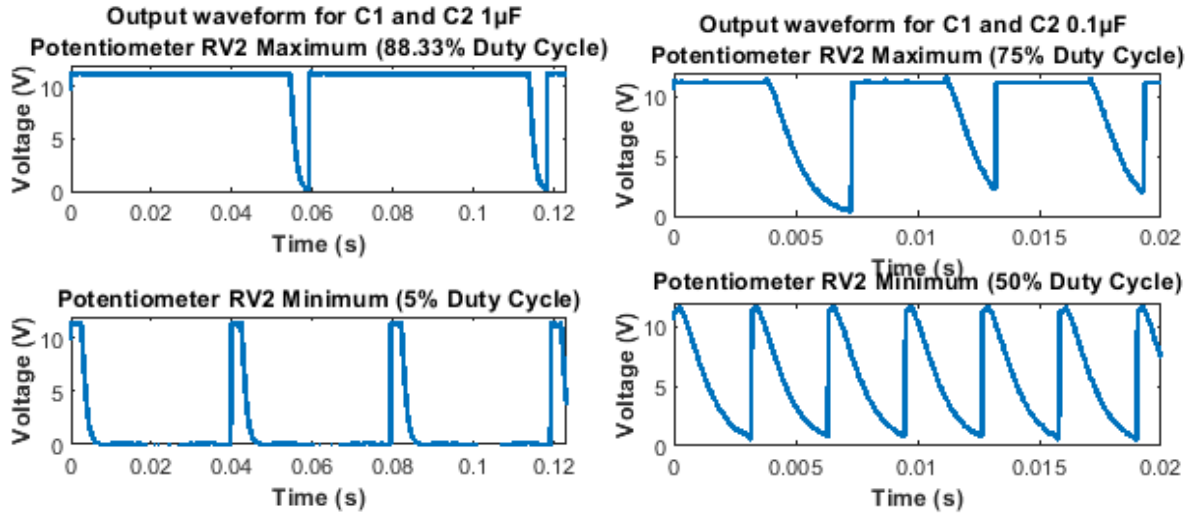


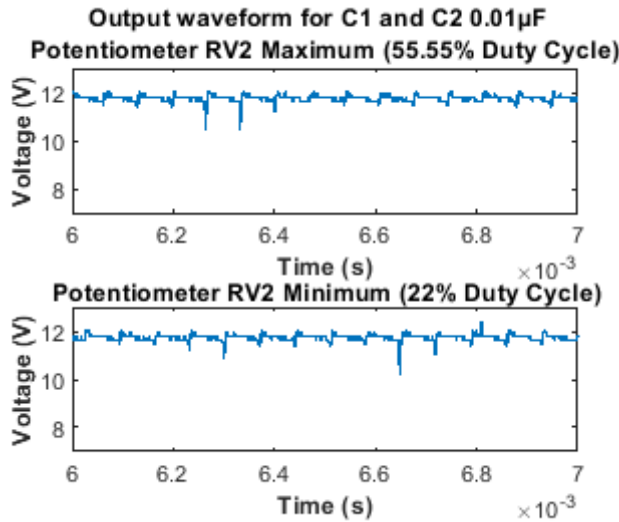
Figure 11: Experimental results of pulse generator for C_1 and C_2 equal to (a) $1 \mu\text{F}$ (b) $0.1 \mu\text{F}$, and (c) $0.01 \mu\text{F}$ when varies the potentiometer RV_1

The result obtained from the experimental result was shown in Figure 12. The pulse width of the output generator circuit was measured when varies the potentiometer RV_2 to the minimum value by adjusted the capacitor C_1 and C_2 equal to $1 \mu\text{F}$, $0.1 \mu\text{F}$, and $0.01 \mu\text{F}$. As can be seen, the pulse generator during ON state will short and the duty cycle is decreased if the value of RV_2 is decreasing. The pulse will lower by decreasing the value of capacitor $0.01 \mu\text{F}$ followed by the $0.1 \mu\text{F}$ and $1 \mu\text{F}$.



(a)

(b)

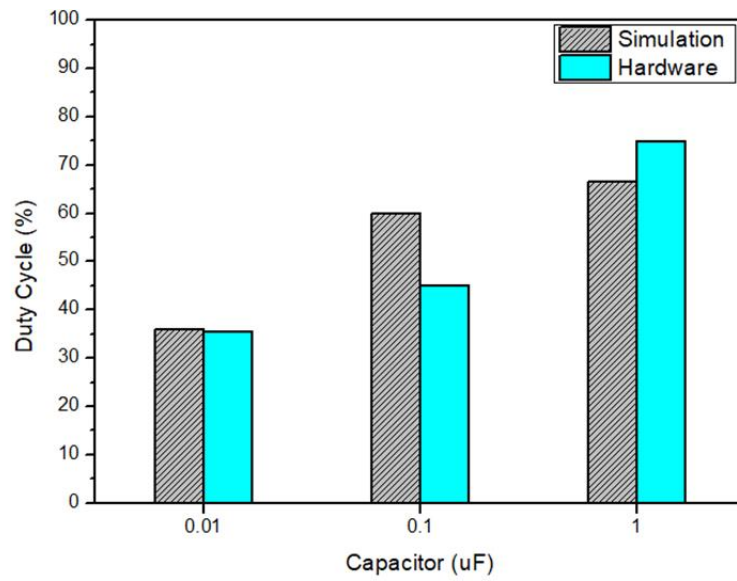


(c)

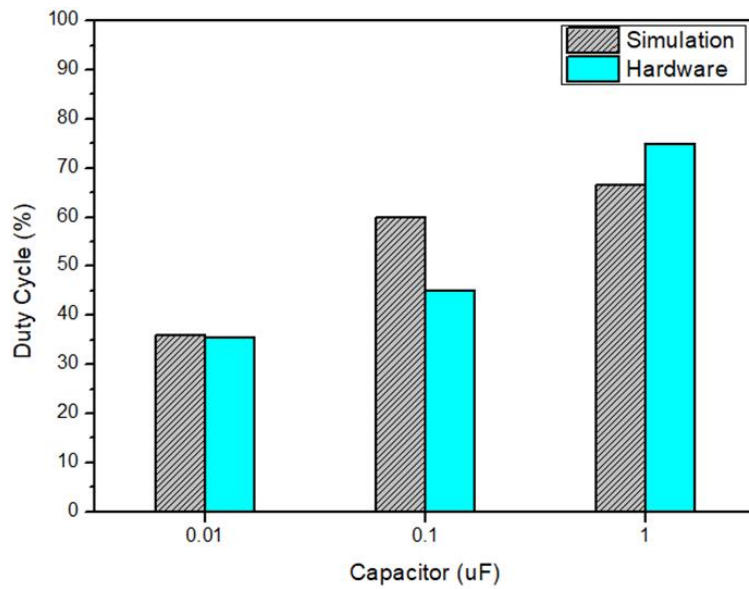
Figure 12: Experimental results of pulse generator waveform for C_1 and C_2 equal to (a) $1\mu\text{F}$ (b) $0.1\mu\text{F}$, and (c) $0.01\mu\text{F}$ when varies the potentiometer RV_2

3.4 Comparison between software and experimental results

Figure 13 and 14 show the duty cycle for frequency and pulse width each capacitor when potentiometer (RV_1 and RV_2) varied at minimum and maximum value for both simulation and hardware. The comparisons were made based on duty cycle information because duty cycle was extracted from pulse width and frequency graph from the previous section. As clearly be seen, all the results matched with the simulated output except that a small drop in the final output voltage was observed which is as expected due to various losses in the circuit.

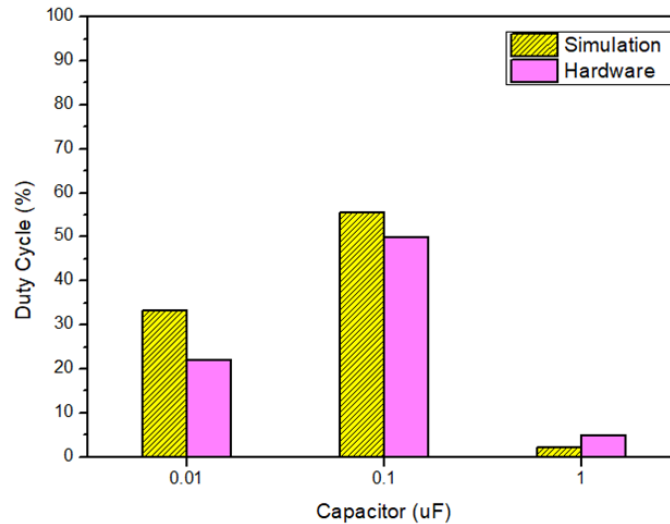


(a)

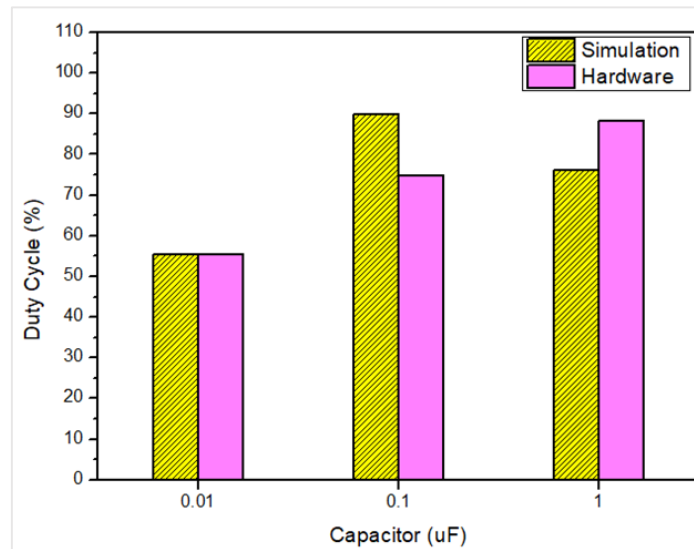


(b)

Figure 13: Duty cycle for each capacitor varied at, a) minimum potentiometer (RV_1) and b) maximum potentiometer (RV_1) for both simulation and hardware.



(a)



(b)

Figure 14: Duty cycle for each capacitor varied at, a) minimum potentiometer (RV₂) and b) maximum potentiometer (RV₂) for both simulation and hardware.

The percentage difference for 0.01 μF , 0.1 μF and 1 μF capacitors when varies RV₁ at minimum value are 2.86 %, 13.69 % and 12.50 % respectively. While RV₁ varies at maximum value, the percentage different for 0.01 μF , 0.1 μF and 1 μF capacitors are 1.4 %, 33.33 % and 14.5 % respectively. For percentage difference when varies RV₂ at minimum value are 33.99 %, 9.99 % and 55.6 % for 0.01 μF , 0.1 μF and 1 μF capacitors. While varies RV₂ at maximum value, the percentage difference for 0.01 μF , 0.1 μF and 1 μF capacitors are 0 %, 16.67 % and 15.93 % respectively. The difference percentage between simulation and hardware occurred might be due to the component stack-up tolerance. Thus, this phenomenon will cause the hardware results slightly different with the simulation.

4. Conclusion

In a conclusion, the portable and adjustable high voltage pulse generator was successfully developed. The pulse generator was developed by using two NE555 timer to chop the electricity into pulses. The first timer controls the frequency and determines how often the pulses occur. While the

second timer control the pulse width by determines the duration of pulse it produces during ON state. Then, the output pulse from the driving circuit is fed into the negative terminal of the ignition coil. The spark is successfully produced on the output ignition coil. That means the voltage obtained by the circuit is enough high to energize the ignition coil.

From the simulation, the effect of tuning the capacitor and resistor value on the output frequency of pulse circuit by using Proteus simulation also has been analyzed. The number of pulses is increased and the duration of pulses during ON state is short by applied the 0.01 μF followed by the 0.1 μF and 1 μF . The smallest value of capacitor gives lower pulse duration and higher output frequency. Both timer U_1 and U_2 consist of 50 k Ω potentiometers. Thus, the timing parameters of the resulting pulses changes by adjusting both potentiometers. The different values of selected capacitors and resistor give a different result of the output frequency of the circuit.

Besides that, the output of the high voltage pulse generator result obtained was validated by comparing it with the simulation and hardware implementation. All the results matched perfectly with the simulated output except that a small drop in the final output voltage was observed which is as expected due to various losses in the circuit. The circuit completely depends on the value of the capacitor and resistor network for variation of pulse frequency and pulse duration. The result of the circuit shows that the circuit can be used to generate high impulse voltages.

Acknowledgement

The authors would like to thank Faculty of Engineering Technology, Universiti Tun Hussein Onn Malaysia for its support.

References

- [1] U. Kogelschatz, "Dielectric-barrier Discharges : Their History , Discharge Physics , and Industrial Applications," vol. 23, no. 1, pp. 1–46, 2003.
- [2] T. Bernhardt, M. L. Semmler, M. Schäfer, S. Bekeschus, S. Emmert, and L. Boeckmann, "Plasma Medicine: Applications of Cold Atmospheric Pressure Plasma in Dermatology," *Oxid. Med. Cell. Longev.*, vol. 2019, pp. 10–13, 2019, doi: 10.1155/2019/3873928.
- [3] H. E. Wagner, R. Brandenburg, K. V. Kozlov, A. Sonnenfeld, P. Michel, and J. F. Behnke, "The barrier discharge: Basic properties and applications to surface treatment," *Vacuum*, vol. 71, no. 3 SPEC., pp. 417–436, 2003, doi: 10.1016/S0042-207X(02)00765-0.
- [4] N. Sahari *et al.*, "The structural analysis of MWCNTs modified by DBD plasma and electrical properties on schottky diode application," *Int. J. Adv. Trends Comput. Sci. Eng.*, vol. 9, no. 1.4 Special Issue, pp. 503–511, 2020, doi: 10.30534/ijatcse/2020/7191.42020.
- [5] A. Chirokov, A. Gutsol, and A. Fridman, "Atmospheric pressure plasma of dielectric barrier discharges *," vol. 77, no. 2, pp. 487–495, 2005, doi: 10.1351/pac200577020487.
- [6] U. Kogelschatz, B. Eliasson, and W. Egli, "From ozone generators to flat television screens: History and future potential of dielectric-barrier discharges," *Pure Appl. Chem.*, vol. 71, no. 10, pp. 1819–1828, 1999, doi: 10.1351/pac199971101819.
- [7] W. Jiang, K. Yatsui, K. E. N. Takayama, S. Rukin, V. Tarasenko, and A. Panchenko, "Compact Solid-State Switched Pulsed Power and," vol. 92, no. 7, 2004.